NONLINEAR INTERACTIONS IN COMBUSTION INSTABILITIES COUPLED BY AZIMUTHAL ACOUSTIC MODES

D. Durox *[1,2], J.F. Bourgouin[1,2], J.P. Moeck[3], M. Philip[1,2], T. Schuller[1,2], S. Candel[1,2]

[1] CNRS, UPR 288, Laboratoire d'Energétique Moléculaire et Macroscopique, Combustion (EM2C)
Grande Voie des Vignes, 92290 Châtenay-Malabry, France
[2] Ecole Centrale Paris, Grande Voie des Vignes, 92290 Châtenay-Malabry, France
[3] Chair of Fluid Dynamics, Hermann-Föttinger-Institut
TU Berlin, Müller-Breslau-Str. 8, 10623 Berlin, Germany
* Corresponding author: daniel.durox@ecp.fr

Annular combustors like those used in gas turbines may give rise to various types of combustion instabilities, and more specifically to oscillations coupled by azimuthal modes. While instabilities coupled by longitudinal modes have been extensively investigated in the past those coupled by azimuthal modes are less well documented. It is then useful to reproduce such oscillations in a laboratory scale system allowing detailed pressure measurements and high speed visualization of the flame motion. To better analyze this phenomenon, it is interesting to have a system capable of presenting instabilities, which reach a stable limit cycle, and feature the same mode for an extended period of time. The present investigation concerns the analysis of an azimuthal instability coupled by a standing mode. This is accomplished with a system comprising an annular plenum feeding sixteen laminar multipoint injectors confined by two cylindrical quartz tubes open to the atmosphere. This device allows full optical access to the combustion region. Eight waveguide microphones are used to simultaneously record the pressure signal at the combustor injection plane and in the plenum. High speed imaging of light emission from the flames provides instantaneous flame patterns. Calculations based on a Helmholtz solver provide a suitable estimate of the frequency observed experimentally and reveal the modal structures corresponding to the observed modes. It is shown that the azimuthal mode is generated in the plenum, but visible also in the chamber, while the longitudinal mode is sustained in the combustion chamber and visible at a reduced level in the plenum. The frequency of this mode is nearly double that of the azimuthal mode. The analysis indicates that positive Rayleigh source terms feed energy to the fundamental and second harmonic components giving rise to highly nonlinear pressure and heat release rate signals in the combustion chamber.

1 Introduction

It is well known that the lean-premixed mode of combustion used in modern gas turbines is particularly likely to generate combustion instabilities [1,2]. Operation under lean conditions and the relatively high energy density associated with the compact flame region promotes the development of oscillations. The modern combustors also do not feature perforated liners and their damping characteristics are reduced [1, 2]. In the annular geometry which is typically adopted in many practical systems, one finds in addition to longitudinal instabilities, oscillations coupled by azimuthal modes [3–5]. During the last period of time several research groups have begun working on instabilities in such annular

configurations. There is a large number of theoretical investigations like that of Krüger *et al.* [6]. These authors use a network of acoustic elements for the calculation of the pressure field in the combustion chamber. It is suggested that control could be achieved by changing the impedance of some burners to detune the system. Stow and Dowling [7] propose a network of compact elements to represent the acoustic response of an annular chamber by assuming that the annulus thickness is small compared to the chamber diameter. The low order model of a generic annular configuration developed by Evesque and Polifke [8] comprises a plenum, a finite number of burners, and a combustion chamber. It is shown that the flow in the injectors hardly alters the acoustic modes, provided that the Mach number is low. Standing azimuthal modes are described, but it is noted that spinning modes could also be considered. Each burner response can be treated separately allowing investigations of different solutions to reduce instability, based for example on symmetry breaking. In the time-domain analysis of Pankiewitz and Sattelmayer [9], the nonlinear flame response was represented by adopting the model suggested by Dowling [10]. An unstable mode with a 1A-1L structure is observed, which is purely spinning without mean flow, and is standing with flow, although the latter is largely subsonic. Small variations seem to play a major role on the nature of the unstable modes observed. Evesque *et al.* [11] define a spin ratio, based on acoustic energetic considerations, to describe the azimuthal acoustic modes in the annular combustors. It is found that the presence of the flow has no influence on the spin ratio and as in [9], it is observed that small changes, such as asymmetries in the pressure field can lead to spinning modes or standing modes. A time-domain approach is also exploited by Morgans et Stow [12], to derive solutions which could be used to test control schemes based on fuel injection modulation. The self-sustained azimuthal acoustic modes are found to be spinning when all burners are identical, but become standing when the symmetry is broken. In the acoustic network model proposed by Schuermans *et al.* [13], the flame is represented by incorporating simplified transfer functions derived from experimental tests, a model which is further refined in Schuermans *et al.* [14]. When the burners are identical, it is shown that at the beginning of the azimuthal instability, the mode is standing, but that as the the calculation proceeds, the mode starts to spin. It is argued that this behavior is due to the nonlinearity in the heat release response to flow perturbations. Prediction of instabilities in a real engine attempted more recently by the same team [15] relies on measured transfer functions of a burner operating under high pressure conditions. The model was also used to confirm the stabilizing effect observed when fuel staging is augmented. Effects of burner staging are considered by Noiray *et al.* [16] where changes in the flame dynamics are introduced without impairing the reduced level of NOx emissions. When the transfer functions of the different burners are uniformly distributed, it is found that the azimuthal instability tends to be spinning but that it evolves into a standing mode when the source terms respond in a nonuniform fashion. In between, the limit cycle involves a mixed standing and spinning mode. In industrial annular combustors, unstable modes switch from time to time between spinning and standing modes. To investigate this phenomenon, Noiray and Schuermans [17] have added to their previous model [16] a background noise which represents the effect of turbulence intensity which stochastically disturbs the amplitude of the limit cycles. It is shown that this assumption is sufficient to explain the random switching between the spinning and standing modes.

Some recent investigations of the problem have relied on numerical solutions of the Helmholtz equation in simple or more complex geometries. A forcing term is incorporated to represent fluctuations in heat release rate induced by the perturbed field [18, 19]. Calculations indicate that the flame transfer function and the boundary conditions have a strong impact on the prediction accuracy. Available computing power also allows large eddy simulations (LES) of unstable modes as exemplified in the case of an annular combustor [20, 21]. It is concluded in [20] that in the configuration investigated the main effect of the azimuthal mode is to induce axial fluctuations of the flow rates passing through the injectors with little interaction between the flames. LES can be used to determine the dynamics of azimuthal instabilities and examine changes in the flame response which might achieve stable operation [22]. In this study, with highly turbulent swirling flames, it is shown that the first azimuthal mode of the annular chamber is unstable. With a hundred cycles calculated, the authors show that the mode which is essentially standing features a slow rotation of the nodal line, but there are many excursions towards a spinning mode, because of turbulent fluctuations. In the standing mode, the velocity of rotation of the nodal line approximately corresponds to the mean velocity induced in the chamber annulus by the swirled flows at the injector outlets.

While the number of theoretical and numerical studies is relatively large, experiments on well instrumented annular systems are less common. One finds however some reports of experimental work carried out on a real gas turbine combustors such as that proposed by Krebs *et al.* [5] which includes pressure measurements in the combustion chamber during sustained oscillations. The azimuthal acoustic mode switched from a standing to a pure spinning mode, and vice versa. This paper contains two records for this situation, but there are no indications on the dynamics of this spinning/standing transition. Azimuthal instabilities are also explored by Moeck *et al.* [23] in an idealized system comprising an annular chamber equipped with 12 injection channels operating as Rijke tubes. These devices are used to simulate injector units but the flame is replaced by electrically heated grids. Also, the Rijke tubes suck air from the surrounding atmosphere and there is no plenum or upstream manifold. This device features two types of oscillations coupled by azimuthal modes which depend on the electrical power put in the system. One of the modes was purely standing, while the other could not be precisely defined as standing or spinning, probably because this mode was a mixed one. Staging in the heating tubes was tested to see if this could reduce or suppress the oscillation but it was found that some modes could be attenuated, while others were strengthened. An interesting model scale annular combustor, which has some features in common with the present geometry, was recently tested by Worth and Dawson [24,25]. This device has a relatively small chamber diameter of 170 mm. Experiments were carried out with 12, 15 or 18 units. Injectors are swirled but their exhaust is obstructed by a central bluff-body which occupies 50% of the outlet and the swirl number is probably moderate due to the axial acceleration of the flow in the annulus around the central body. To obtain azimuthal instabilities, the chamber had to be operated with a mixture of ethylene and air, and the inner chamber wall had to be made shorter than the outer wall (130 mm and 170 mm respectively). For equivalence ratios above 0.85, a strong azimuthal instability was observed, involving a spinning or standing wave depending on the spacing between injectors and the swirl direction. Of the six conditions investigated, four cases are essentially standing, one is flipping between spinning and standing, and the sixth case features a bimodal probability, with a small peak corresponding to the standing state and a higher peak pertaining to a spinning wave. When the two modes co-exist switching takes place between them. It is also found that the instability is enhanced when the flames are closely packed (when the injector spacing is reduced) giving rise to strong interactions between adjacent reactive layers.

Another annular configuration called MICCA is investigated by our team at EM2C, CNRS. Dynamics of ignition and light around in this combustor is investigated by Bourgouin *et al.* [26]. The device is equipped with an annular plenum having a rectangular section which delivers premixed reactants to 16 swirling injectors. The chamber walls are transparent providing full optical access. Experiments [27] carried out with swirled injectors equipped with an outlet flare, indicate that the system exhibits longitudinal and azimuthal instabilities depending on operating conditions. In the latter case, the oscillation evolves continuously from a spinning to a standing mode, the standing motion being more probable than the spinning one. For the longitudinal mode, some of the flames (3 or 4) are nearly in phase opposition with their neighbors but this does not prevent the occurrence of instability.

In summary, one can say that current studies on azimuthal instability predictions do not agree with each other, that theoretical models make some strong assumptions which need to be improved and that comparisons with experimental data are still lacking. This is so most probably because it is not easy to incorporate a realistic turbulent swirling flame response in the models.

To circumvent this difficulty the swirled injectors used in [27] are replaced in the present investigation by multipoint injectors generating a set of conical flames. This is accomplished by making use of 16 circular perforated plates. This geometry has the advantage to present a broad frequency dynamic range [28, 29] without the stochastic behavior of turbulent swirled flames. The response can also be represented with a Flame Describing Functions (FDF) and previous studies have shown that the limit cycle amplitudes of longitudinal modes could be suitably retrieved with the unified framework devised in [28,29]. These flames can be used to obtain information on azimuthal unstable modes in the absence of stochastic effects associated with the swirling flames. This provides a database which complements that reported in [27] and may be valuable in the development of theoretical modeling. This article describes the particular case of a robust standing azimuthal mode with a quasi-stationary nodal line.

The manuscript is organized as follows. The experimental annular combustor, diagnostics and data processing methods are described in Section 2. The standing azimuthal instability is presented in Sec-

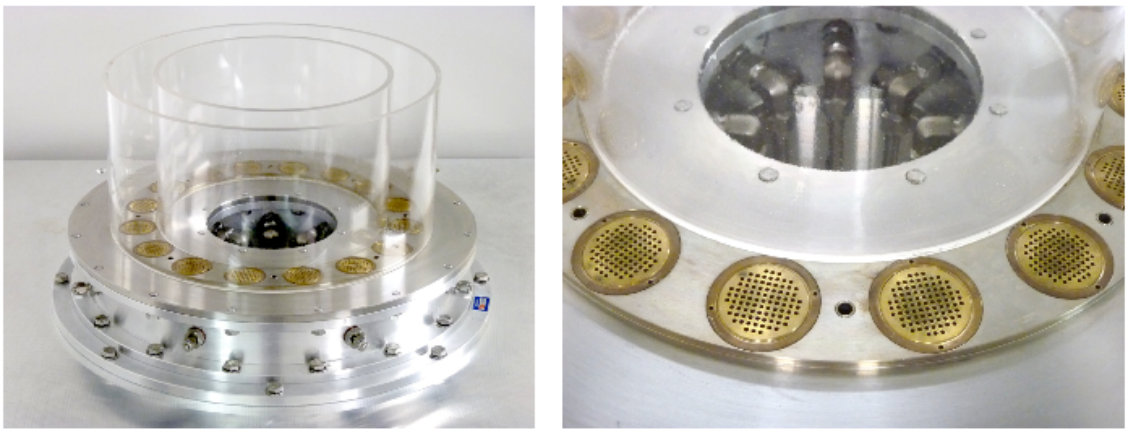

Figure 1: Left, view of the annular combustor MICCA. The annulus mean diameter is 350 mm. The chamber walls are 200 mm in length. Each perforated plate has 89 orifices, 2 mm in diameter arranged on a square mesh of 3 mm in spacing. Each plate is 6 mm thick. The chamber backplane features pressure taps communicating with waveguide microphones. Taps used to measure pressure in the plenum are also visible. Right, details of the perforated plates. The outer wall was removed to avoid reflections. Three pressure taps are visible between the grids.

tion 3. A modal identification is carried out in Section 4 to compare experimental frequencies and numerical estimates. Results are discussed in Section 5.

2 Experimental setup, diagnostics and data processing

Setup

The burner shown in Fig. 1 comprises a horizontal upstream plenum closed at the top by an annular plate with sixteen multipoint injectors and a combustion chamber made of two cylindrical concentric quartz tubes mounted on the horizontal annular plate which serves as a chamber backplane. The diameters of the inner and outer quartz tubes are 300 mm and 400 mm respectively and their length is 200 mm. The quartz tubes allow optical visualization of the flames in the near ultraviolet and visible ranges of the flames formed in this arrangement. Each multipoint injector is made of a circular brass plate, 6 mm thick, comprising 89 channels, 2 mm in diameter, distributed on a square mesh of 3 mm (on the right in Fig. 1).

Air and propane are delivered to a premixing unit. The mixture is then conveyed to an annular plenum through eight channels which are plugged on the internal sides of the annulus (visible in the right image in Fig. 1). Gases in the plenum are exhausted through sixteen multipoint injectors mounted on the flange which separates the plenum from the chamber and constitutes the chamber backplane. The system is ignited by a movable spark plug, which is introduced through the chamber outlet, brought close to the chamber backplane to generate the spark, and is removed after the light around. For a bulk velocity of the mixture $v_0 = 2.12\,\mathrm{m.s^{-1}}$ in each channel of the perforated plates (at ambient temperature and pressure conditions) and for an equivalence ratio $\phi = 1.11$, the experimental setup features a strong azimuthal instability. After a warm-up of about ten minutes, a quasi steady standing mode is established which remains in a steady state for several seconds or even tens of seconds.

Diagnostics

Eight pressure taps are installed at the base of the annular chamber (Fig. 1, right). Each pressure tap is located at an equal distance from two injectors. The pressure tubes pass through the plenum and

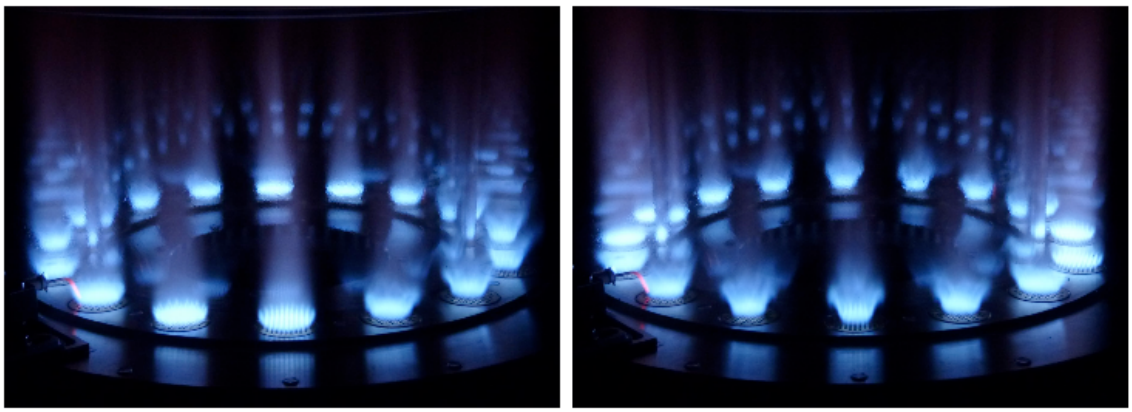

Figure 2: View of the annular combustion chamber in operation, when the system is unstable and features a standing azimuthal acoustic mode. The mode is quasi steady during a period of several seconds. On the left, the nodal line nearly coincides with the vertical axis of the image. On the right, the nodal line has rotated to a position which is nearly horizontal in this image.

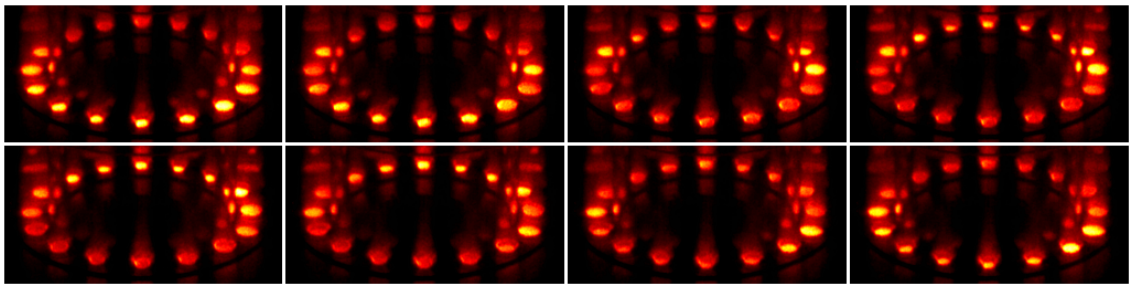

Figure 3: Eight images obtained by phase averaging, showing a complete cycle of flame motion. The reading direction is from left to right and from top to bottom. The nodal line is approximately horizontal in these images.

are terminated by 25 m long waveguide tubes closed at their end. A microphone is flush mounted on each waveguide, at 170 mm from the chamber back plane. The pressure signals are processed by taking into account the propagation delay associated to this distance. Eight other pressure taps are located in the plenum (Fig. 1, left). Eight microphones were used for this experiment, and they were plugged to the various pressure taps, depending on the data that were desired. Measurements of heat release rate were made with two photomultipliers equipped with suitable filters passing the light radiated by OH^* radicals. The field of view of the photomultipliers has been spatially restricted and it can be reasonably assumed that the photomultiplier signals correspond to the global heat release rate of the flame that it is pointing to. It is recognized that the radiation of OH^* constitutes a good tracer of the heat release rate for premixed flames [30, 31]. The pressure and photomultiplier signals are acquired with a computer equipped with an analog to digital converter controlled by the LabVIEW software. For each test, the sampling rate was 32768 Hz during 4 or 8 s.

Camera

High speed films are recorded by an intensified CMOS camera APX-i2 at a resolution of $512 \times 256\,\mathrm{px}^2$ with an 8-bit resolution in grey levels. To get a complete view of the annular chamber, the camera is equipped with a Nikon 35-200 mm zoom and was set at 3.5 m from the center of the combustion cham-

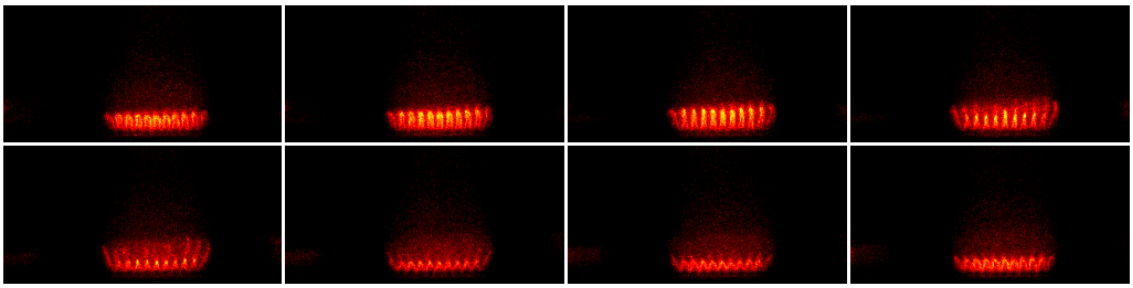

Figure 4: One cycle of oscillation for a multipoint injector located in the vicinity of the nodal line. The reading direction is from left to right and from top to bottom.

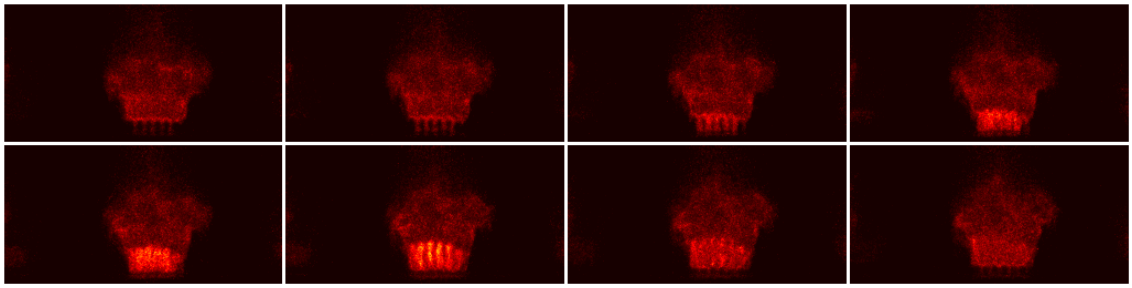

Figure 5: One cycle of oscillation for a multipoint injector located at 90° from the nodal line. This injector is close to a pressure antinode. The reading direction is from left to right and from top to bottom.

ber. A precise view of the flame motion is obtained with a Nikon 60 mm lens and the camera is approached at a distance of 1.50 m from the center. The frame rate and shutter speed are respectively set at 12500 Hz and 79 μs. The amplifier gain remains fixed for all experiments discussed in this study. The camera is sensitive to radiation in the visible and UV ranges down to $\lambda \simeq 200$ nm. However, the UV radiation is greatly filtered by the optical lenses of the camera made of glass. The light intensity recorded by the camera is assumed to be dominated by the emission of excited radicals in the visible domain, mainly from CH^* and C_2^* radicals. The color of the premixed flame is light blue and, for an equivalence ratio around $\phi = 1.1$ the soot production is negligible (see Fig. 2). Images recorded by this device can therefore be interpreted as representative of the instantaneous heat release rate [30, 31].

3 Standing azimuthal instability

Flame dynamics

Two images, taken with a long time exposure, are shown in Fig. 2, during unstable operation. The left shows that the nodal line is nearly vertical in the image. In the vicinity of this line, the flames are more compact, hung on the surface of the perforated plate and take the form of a collection of small conical flames which are nearly the same during the oscillation cycle, when they are in this quiet condition [28, 29]. Away from the nodal line, the flames are elongated and detached over the edge of the plates. This effect is clearly visible in the right image. The nodal line is roughly horizontal in this case. The flames that are furthest from the nodal line are set into a strong periodic motion. When the mode is standing, it remains in a quasi-stationary position for a long time: a few seconds or more if the flow and equivalence ratio parameters are fixed.
Images recorded by the camera, at a high framerate, can be phase averaged to highlight the flame mo-

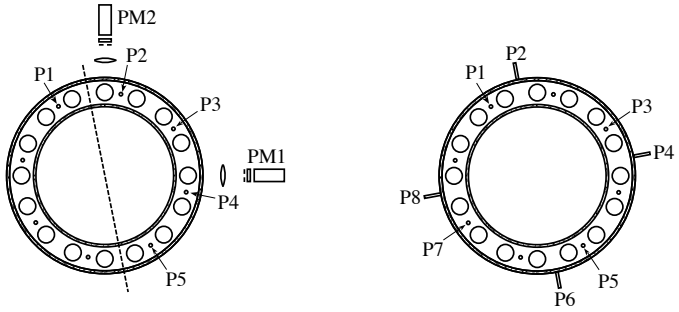

Figure 6: Schematic representation of the chamber backplane showing the microphones and photomultipliers positions. Left: configuration used for the first data set. The dashed line roughly corresponds to the nodal line observed during the first group of experiments. Right: Sketch of the system base showing positions of microphones P1-P3-P5-P7 in the backplane and positions of microphones P2-P4-P6-P8 in the plenum used to acquire the second data set.

tion. As will be seen later, the main frequency of oscillation is at 495 Hz, and phase averaging can be performed with this reference frequency. A complete cycle is shown in Fig. 3. The nodal line is almost horizontal in these images, and one can distinguish a tilting motion around this line. The flames, which are located near the nodal line are still quite bright and cover a large horizontal surface as their motion is weak.

Although the nodal line can be clearly identified, it is found that the flames, which are close to it, are not perfectly steady. It is possible to examine this motion as well as that of the flames which are in the orthogonal direction and feature flames with the largest amplitudes of motion. These visualizations are presented in Figs. 4 and 5. In Fig. 4, the flames move at the fundamental frequency of the excitation (495 Hz), all together, but with a small amplitude of oscillation. All flames are anchored on the perforated grid. When the flames are far from the nodal line, the flames move together with large amplitudes of oscillation (Fig. 5). During the cycle, the brightness, and therefore the heat release rate, changes dramatically. For example, images 1 and 2 of the sequence are very dark, while images 5 and 6 are quite bright. In image 7, pockets are formed by a pinching process taking place near the flame top. These visualizations, which are characteristic of the standing mode under examination, indicate that the flames are never completely stationary, even in the vicinity of the nodal line. An oscillation is always present. This may be so because the nodal line is located between two injectors, or because the mode is not purely standing. To obtain further information on the process one has to examine the pressure fluctuations and their relationship with the heat release rate oscillations.

Acoustic characterization of the standing mode

Time records of pressure and heat release rate are now used to characterize this unstable mode. A first data set corresponds to the sensors arranged as in Fig. 6, left. Pressures are measured in the combustion chamber, on a semi-circle. The two photomultipliers (PM1 and PM2) are arranged as shown in Fig. 6. They are equipped with a cover, to detect only the light coming from the flame in front of the sensor. A vertical mask is also positioned in the inner quartz tube to stop the light coming from the flame located on the opposite side of the chamber. Typical pressure records are shown in Fig. 7. The raw signals plotted in the top subfigure are periodic but not sinusoidal. In the lower subfigure, the signals are band pass filtered around the first harmonic at 495 Hz (i.e. the fundamental) (on the left) and around the second harmonic (990 Hz) (on the right).

The pressure maximum is detected by P3 and P4 probes, with about 75 Pa in the plot. The raw signals are highly nonlinear. They also differ greatly depending on the sensor position. A closer examination indicates that the P2 and P5 signals are nearly identical, at all instants. This is also the case for the P3 and P4 signals. When the signals are filtered around the fundamental (between 450 and 550 Hz),

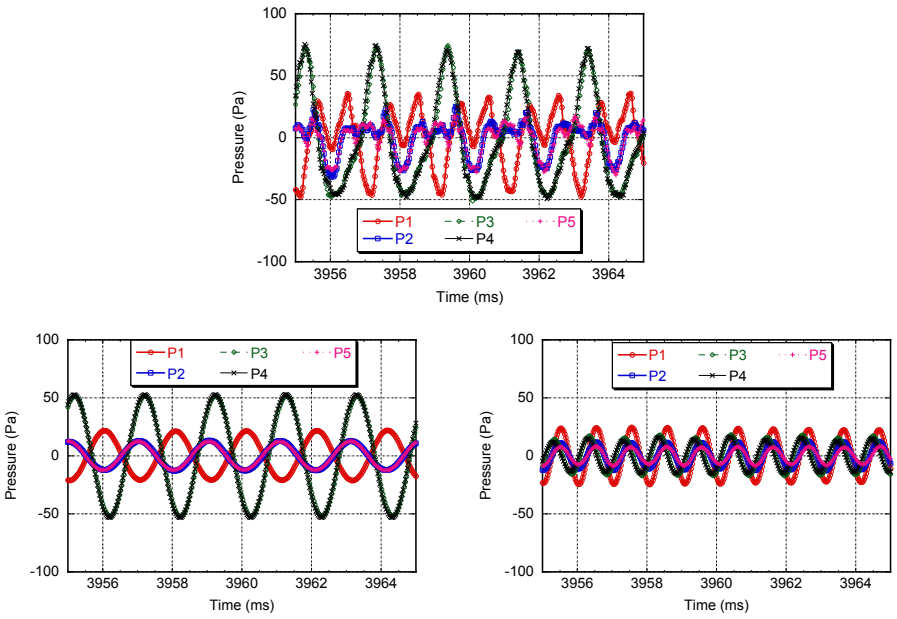

Figure 7: Pressure signals corresponding to the first data set. These diagrams show typical signals recorded during a 4 s sequence. The top subfigures show the raw signals. In the bottom subfigure, left, the signals are band-pass filtered between 450 and 550 Hz. At the bottom, right, the signals are band-pass filtered between 900 and 1100 Hz.

one finds that the P2, P3, P4 and P5 signals are nearly in phase, while the P1 signal is almost in phase opposition with the four others. The signals of the five microphones which have been filtered around the second harmonic (990 Hz) are approximately in phase while their level is lower than that of the fundamental component. This suggests that a longitudinal acoustic wave is also present but with a lower magnitude than that corresponding to the fundamental component at 495 Hz. The waveforms corresponding to the fundamental mode (bottom left in the figure) are typical of a standing mode in the azimuthal direction. It is interesting to examine the phase difference between the pressure signals in the 4 s records, as well as the ratio between the respective amplitudes. These comparisons are based on the cross-spectral densities between the signals at the frequency of the fundamental mode (495 Hz). Results are shown in Fig. 8. In the left plot, it is seen that P3 and P4 signals keep the same amplitude during the 4 s of the recording. P2 and P5 signals have very similar amplitudes. The amplitude of P1 is much lower than that of P3. The phase shifts, shown in the plot on the right, indicate that P2 and P5 signals are in phase, as well as the P3 and P4 signals (the two phase differences Ph (P2->P3) and Ph (P2->P4) are practically superimposed on the graph). There is very little phase shift between P2 and P3. The P1 signal is always out of phase by about π radians. These results indicate that the nodal line passes diametrically between the two injectors located between the pressure taps P1 and P2. There may be a little jitter but the nodal line remained in this neighborhood for the 4 s record.

The signals collected by the two photomultipliers (PM1 and PM2) and two pressure sensors that are closest (P4 and P2), are plotted in the top of Fig. 9. The pressure signals are time shifted, to account for the delay introduced by propagation in the waveguides. The pair of sensors (PM1,P4) and (PM2,P1) are at 90° from each other and the corresponding waveforms are notably different. The heat release rate for the flame viewed by PM2 is practically symmetrical and nearly sinusoidal, in contrast to the PM1 signal, which features a strong asymmetry and a high amplitude of oscillation. The pressure signals P2 and P1 are both nonlinear but the deformation resulting from this nonlinearity is more visible in the P2 signal. The power spectral densities shown in the lower subfigures indicate that the pressure signals are highly nonlinear in the combustion chamber, with the presence of many harmonics of the fundamental component at 495 Hz. It is interesting to note that for the P2 signal, the second harmonic is slightly

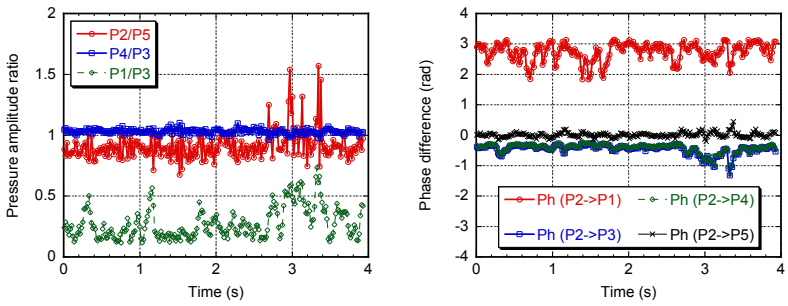

Figure 8: Left : Evolution of the pressure amplitude ratios as a function of time. Right : Evolution of the phase differences as a function of time.

stronger than the fundamental. It should be noted that the pressure signal P4 is roughly in phase with the PM1 signal (top, right in Fig. 9). A more accurate visualization of the phase difference can be obtained by filtering these signals around the fundamental frequency. This is shown in the second row and right column. In the pressure anti-node, the pressure and heat release rate are nearly in phase, verifying the Rayleigh criterion. This can also be confirmed by studying the time evolution of the phase shift between the microphones and photomultipliers filtered signals (Fig. 10). In the region where the pressure amplitude reaches its maximum, which is close to P4, the phase difference with the PM1 signal is nearly constant and equal to 0.5 rad. Thus the Rayleigh source term in the balance of acoustic energy is positive, even if the two signals are not perfectly in phase. In the vicinity of P2, the situation is less clear. The P2 and PM2 signals verify the Rayleigh criterion to a lesser extent. There are even times where the signals are almost in phase opposition. The instability is mainly driven by the flames located near the pressure antinode, i.e. in the region where the pressure amplitude is maximum. It is interesting to look at the behavior of the pressure and heat release rate signals filtered around the second harmonic (around 990 Hz). The evolution of P2 and PM2 (third line in Fig. 9) indicates that the Rayleigh source term is negative indicating that energy is pumped out from the oscillation. In contrast, the signals P4 and PM1 show that there is a significant contribution to the acoustic energy in this region. The corresponding source term outweighs the sink term found near P2 indicating that the oscillation at 990 Hz can be sustained.

It is now interesting to examine the pressure waveforms in the plenum. The microphone positions adopted for this analysis are shown in Fig. 6, right. Four microphones are installed in the combustion chamber and placed at 90° from each other. Four other microphones were flush mounted in the plenum, also at 90° from each other. The results are displayed in Fig. 11. The signals recorded in the combustion chamber (P1, P3, P5, P7) are similar to those described previously. In the plenum, the signals are nearly sinusoidal as exemplified by P4 and P8. These two signals reach large amplitudes, nearly 400 Pa peak and they are in phase opposition. An accurate examination, not shown here, exhibits that a small oscillation at 990 Hz remains in the plenum on the four pressure probes (about 10 Pa peak), with a signature which is roughly that of the longitudinal mode observed in the combustion chamber. The amplitudes of P2 and P6 are almost zero, indicating that the nodal line passes through these two sensors. From this information and from what has been found previously, one can conclude that the main acoustic oscillation (at 495 Hz) is coupled by a standing azimuthal mode established in the plenum.

4 Discussion

To explain the nonlinear behavior of the acoustics in the combustion chamber, it is useful to plot the acoustic modes in the combustion chamber, especially those which are close to the observed frequencies. The calculations are carried out using a Helmholtz solver (Comsol). One assumes a temperature of 300 K in the plenum, and a mean temperature of 1500 K in the combustion chamber. The results are plotted in Fig. 12 for the mode 1A0L, which is essentially an azimuthal mode in the plenum at 482 Hz,

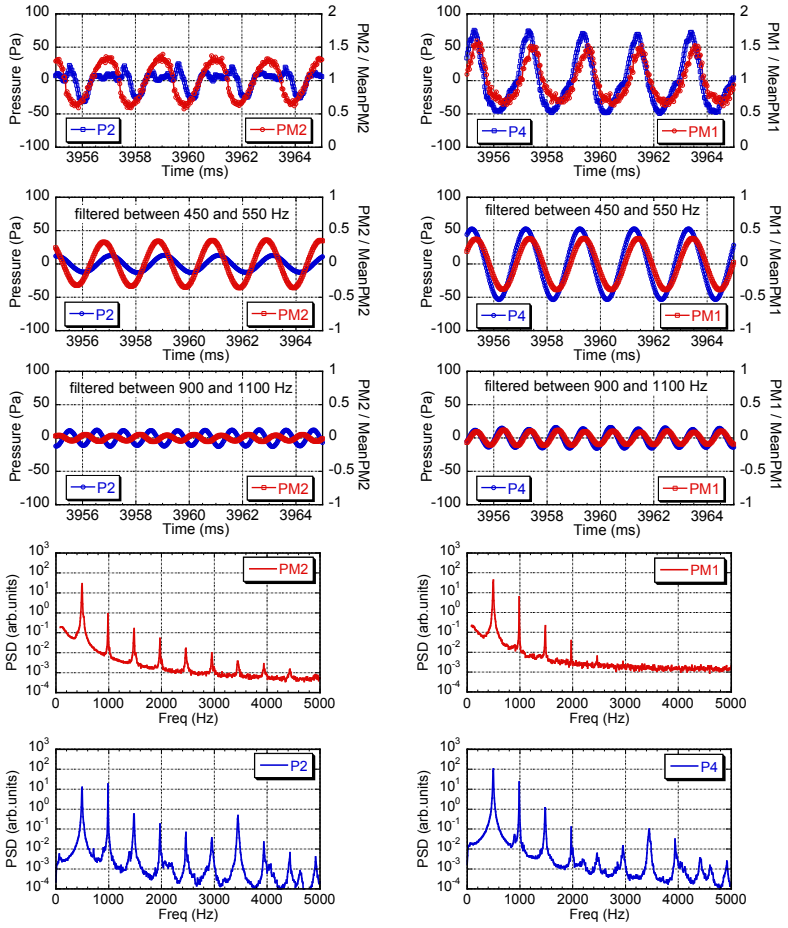

Figure 9: Pressure signals and light intensities measured by sensors P2 and PM2 (left column) and P4 and PM1 (right column). In the second and third rows of subfigures the signals are filtered around the fundamental (the first harmonic) at 495 Hz and around the second harmonic at 990 Hz. The lower row of subfigures show the power spectral densities of the four signals.

and for the 0A1L mode, which is a longitudinal mode at about 969 Hz. These two modal resonances are close to experimental frequencies and their modal structures also match experimental observations. The oscillation at the fundamental frequency is purely azimuthal at a frequency of 495 Hz and this oscillation is observed in the plenum and in the chamber. The oscillation at 990 Hz is mainly found in the chamber and its frequency is close to the 0A1L mode.

The most powerful instability mechanism appears in the plenum. In that cavity, the fundamental prevails, and the amplitude of the pressure oscillations reaches 400 Pa at the pressure antinode. This induces large velocity fluctuations in the multipoint injectors located near the pressure anti-nodal line giving rise to large fluctuations in heat release rate. This flame oscillation at 495 Hz is close to being in phase with the pressure oscillation at the base of the combustion chamber (about 0.5 rad for the phase difference), which delivers energy to the system and maintains the instability coupled by the fundamental mode. In the combustion chamber, in addition to the fundamental mode, one finds a second oscillation at a frequency which corresponds to the second harmonic, but is less energetic and has essentially the same amplitude over the whole periphery of the chamber (Fig. 7 bottom right). The characteristics of this oscillation match those of the 0A1L longitudinal mode. In the selected configuration the calculated frequency of this last mode is nearly twice that of the 1A0L mode. This instability at 990 Hz, is maintained by a coupling of the pressure oscillation at this frequency, with the second harmonic

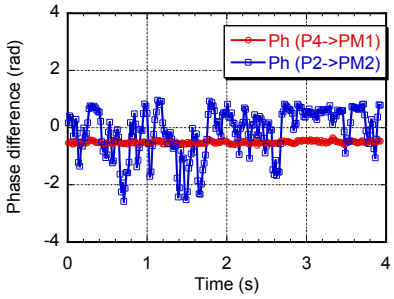

Figure 10: Phase difference between P4 and PM1 and between P2 and PM2 during a 4 s recording.

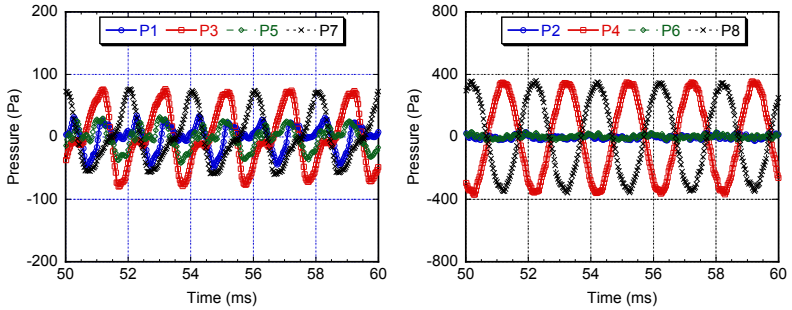

Figure 11: Pressure signals in the chamber (left) and the plenum (right) taken during the second recording of 4 s.

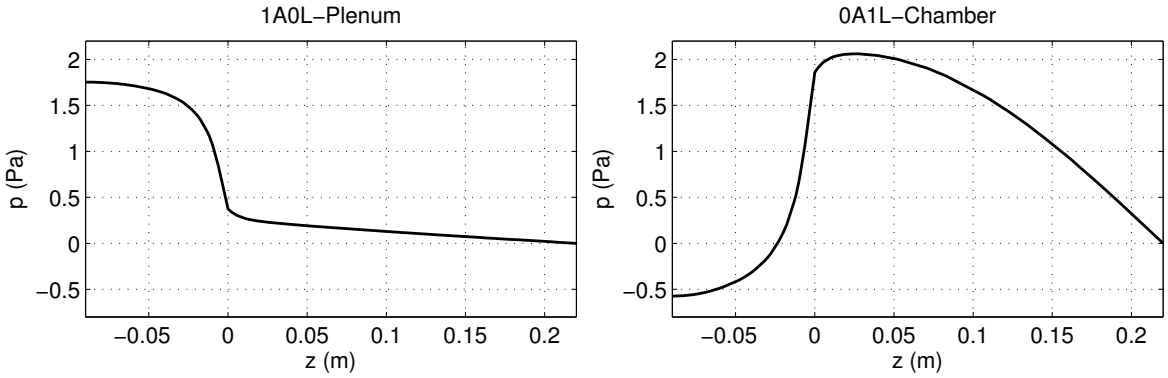

Figure 12: Acoustic mode structures in hot conditions: 300 K in the plenum and 1500 K in the combustion chamber. Left : The first azimuthal mode 1A0L. Right : First longitudinal mode 0A1L. The coordinate z is along the axial direction. z = 0 corresponds to the combustion chamber backplane.

of the heat release rate oscillation as can be deduced from Fig. 9 (left column, third row). The second harmonic of the heat release rate is nearly in phase with the second harmonic of the pressure thus providing energy to the pressure oscillation at 990 Hz. Inside the combustion chamber, the combination of the azimuthal mode localized in the plenum, which resonates at a low frequency, with a longitudinal mode at the double frequency, leads to strongly nonlinear pressure signals. This special combination arises because the plenum and combustion chamber are strongly coupled, and because the two instabilities have frequencies which are related by a factor of 2. Since the heat release rate in the flames is

also nonlinear [28, 29], it can drive the two resonances simultaneously.

One question that has not been addressed concerns the orientation of the nodal line. In the present study, the nodal line is always in the same position, and one may wonder why in view of the perfect symmetry of the system. Systematic tests and many improvements were made to the experimental setup to minimize the asymmetries but without any change in the nodal line location. Other tests, not presented in this article indicate that, for a set of operating conditions which slightly differ from that used in the present investigation, one observes two types of situations involving a standing azimuthal mode. In the first one, the nodal line rotates abruptly by 90° with respect to the nodal line passing through P2-P6 (Fig. 6, right) before suddenly returning to its initial position. The system switches randomly two or three times every ten seconds. In a second situation obtained by changing slightly the operating conditions, one observes a rapid and random succession of changes in nodal line position. This takes place every one to two seconds, and the nodal line moves to a different angle after each transition. In these two situations, the standing mode appears to be a characteristic state of the present configuration and the location and transient motion of the nodal line is linked to the flow conditions, equivalence ratio and coupling between the plenum and combustion chamber but not to an obvious geometrical asymmetry of the combustor injector arrangement.

5 Conclusion

This article is concerned with instabilities in annular combustion systems comprising a periodic arrangement of injectors. The laboratory scale configuration allows a full optical access to the flames and it is equipped with pressure sensors flush mounted in the plenum and waveguide microphones communicating with the chamber backplane. The analysis focuses on a self-sustained combustion instability of a standing mode which is coupled by an azimuthal mode. It is found that the pressure and heat release signals in the chamber are highly nonlinear while the pressure signals in the plenum are nearly sinusoidal. A detailed analysis indicates that the azimuthal mode is generated in the plenum, at the fundamental frequency observed in the experiment, while a longitudinal mode is also present in the combustion chamber and at a reduced level in the plenum. The frequency of this mode is nearly double that of the azimuthal mode. It is suggested that this combination of modes is a result of the nonlinear response of the flame which generates heat release fluctuations at the fundamental and second harmonic frequencies which correspond to the eigenmodes 1A0L and 0A1L of this system. The analysis indicates that positive Rayleigh source terms are formed by pressure and heat release fluctuations which are in phase at the two modal frequencies and feed energy to the fundamental and second harmonic components giving rise to the observed highly nonlinear pressure and heat release rate signals in the combustion chamber.

References

[1] J.J. Keller. Thermoacoustic oscillations in combustion chambers of gas turbines. *AIAA Journal*, 33(12):2280–2287, December 1995.

[2] J.R. Seume, N. Vortmeyer, W. Krause, J. Hermann, C.-C. Hantschk, P. Zangl, S. Gleis, D.A. Vortmeyer, and A. Orthmann. Application of active combustion instability control to a heavy duty gas turbine. *Journal of Engineering for Gas Turbines and Power*, 120(4):721–726, 1998.

[3] U. Krüger, J. Hüren, S. Hoffmann, W. Krebs, and D. Bohn. Prediction of thermoacoustic instabilities with focus on the dynamic flame behavior for the 3A-series gas turbine of Siemens KWU. In *Proceedings of ASME Turbo Expo 1999*, number 99-GT-111, 1999.

[4] B. Schuermans, W. Polifke, and C. Paschereit. Modeling transfer matrices of premixed flames and comparison with experimental results. In *Proceedings of ASME Turbo Expo 1999*, number 1999-GT-0132, Indianapolis, USA, 1999.

[5] W. Krebs, P. Flohr, B. Prade, and S. Hoffmann. Thermoacoustic stability chart for high-intensity gas turbine combustion systems. *Combustion Science and Technology*, 174(7):99–128, 2002.

[6] U. Krüger, J. Hüren, S. Hoffmann, W. Krebs, P. Flohr, and D. Bohn. Prediction and measurement of thermoacoustic improvements in gas turbines with annular combustion systems. *Journal of Engineering for Gas Turbines and Power*, 123:557–566, 2001.

[7] S.R. Stow and A.P. Dowling. Thermoacoustic oscillations in an annular combustor. In *Proceedings of ASME Turbo Expo 2001*, number GT2001-0037, New Orleans, USA, June 8-11, 2001.

[8] S. Evesque and W. Polifke. Low-order modelling for annular combustors: validation and inclusion of modal coupling. In *Proceedings of ASME Turbo Expo 2002*, number GT-2002-30064, Amsterdam, The Netherlands, june 3-6 2002.

[9] C. Pankiewitz and T. Sattelmayer. Time domain simulation of combustion instabilities in annular combustors. In *Proceedings of ASME Turbo Expo 2002*, number GT-2002-30063, Amsterdam, The Netherlands, June 3-6, 2002.

[10] A.P. Dowling. Nonlinear self-excited oscillations of a ducted flame. *Journal of Fluid Mechanics*, 346:271–290, 1997.

[11] S. Evesque, W. Polifke, and C. Pankiewitz. Spinning and azimuthally standing acoustic modes in annular combustors. In *9th AIAA/CEAS Aeroacoustics Conference and Exhibit*, Hilton Head, South Carolina, USA, 12-14 May 2003.

[12] A.S. Morgans and S.R. Stow. Model-based control of combustion instabilities in annular combustors. *Combustion and Flame*, 150:380–399, 2007.

[13] B. Schuermans, V. Bellucci, and C.O. Paschereit. Thermoacoustic modeling and control of multi-burner combustion systems. In *Proceedings of ASME Turbo Expo 2003*, number GT-2003-38688, Atlanta, Georgia, USA, June 16-19 2003.

[14] B. Schuermans, C.O. Paschereit, and P. Monkewitz. Non-linear combustion instabilities in annular gas-turbine combustors. In *44th AIAA Aerospace Sciences Meeting and Exhibit*, number 2006-0549, Reno, NV, USA, January 9-12, 2006.

[15] B. Schuermans, F. Guethe, D. Pennel, G. Guyot, and C. Paschereit. Thermoacoustic modeling of a gas turbine using transfer functions measured under full engine pressure. *Journal of Engineering for Gas Turbines and Power*, 132(111503), November 2010.

[16] N. Noiray, M. Bothien, and B. Schuermans. Investigation of azimuthal staging concepts in annular gas turbines. *Combustion Theory and Modelling*, 15(5):585–606, 2011.

[17] N. Noiray and B. Schuermans. On the dynamic nature of azimuthal thermoacoustic modes in annular gas turbine combustion chambers. *Proceedings of the Royal Society*, 469(2151):20120535, 2013.

[18] F. Nicoud, L. Benoit, C. Sensiau, and T. Poinsot. Acoustic modes in combustors with complex impedances and multidimensional active flames. *AIAA Journal*, 45(2), February 2007.

[19] S.M. Camporeale, B. Fortunato, and G. Campa. A finite element method for three-dimensional analysis of thermo-acoustic combustion instability. *Journal of Engineering for Gas Turbines and Power*, 133(011506), January 2011.

[20] G. Staffelbach, L.Y.M. Gicquel, G. Boudier, and T. Poinsot. Large eddy simulation of self-excited azimuthal modes in annular combustors. *Proceedings of the Combustion Institute*, 32(2):2909–2916, 2009.

[21] P. Wolf, R. Balakrishnan, G. Staffelbach, L.Y.M. Gicquel, and T. Poinsot. Using LES to study reacting flows and instabilities in annular combustion chambers. *Flow Turbulence and Combustion*, 88:191–206, 2012.

[22] P. Wolf, G. Staffelbach, L.Y.M. Gicquel, J.-D. Müller, and T. Poinsot. Acoustic and large eddy simulation studies of azimuthal modes in annular combustion chambers. *Combustion and Flame*, 159:3398–3413, 2012.

[23] J.P. Moeck, M. Paul, and C.O. Paschereit. Thermoacoustic instabilities in an annular Rijke tube. In *Proceedings of ASME Turbo Expo 2010*, number GT2010-23577, Glasgow, UK, June 14-18, 2010.

[24] N.A. Worth and J.R. Dawson. Self-excited circumferential instabilities in a model annular gas turbine combustor: global flame dynamics. *Proceedings of the Combustion Institute*, 34:3127–3134, 2013.

[25] N.A. Worth and J.R. Dawson. Modal dynamics of self-excited azimuthal instabilities in an annular combustion chamber. *Combustion and Flame*, submitted.

[26] J.F. Bourgouin, D. Durox, T. Schuller, J. Beaunier, and S. Candel. Ignition dynamics of an annular combustor equipped with multiple swirling injectors. *Combustion and Flame*, 160:1398–1413, 2013.

[27] J.F. Bourgouin, D. Durox, J.P. Moeck, T. Schuller, and S. Candel. Self-sustained instabilities in an annular combustor coupled by azimuthal acoustic modes. In *Proceedings of ASME Turbo Expo 2013*, number GT2013-95010, San Antonio, Texas, USA, June 3-7, 2013.

[28] N. Noiray, D. Durox, T. Schuller, and S. Candel. A unified framework for nonlinear combustion instability analysis based on the flame describing function. *Journal of Fluid Mechanics*, 615:139–167, 2008.

[29] F. Boudy, D. Durox, T. Schuller, and S. Candel. Nonlinear mode triggering in a multiple flame combustor. *Proceedings of the Combustion Institute*, 33, Issue1:1121–1128, 2011.

[30] I.R. Hurle, R.B. Price, T.M. Sugden, and A. Thomas. Sound emission from open turbulent premixed flames. *Proceedings of the Royal Society of London. Series A, Mathematical and Physical Sciences*, 303:409–427, 1968.

[31] R. Price, I. Hurle, and T. Sugden. Optical studies of the generation of noise in turbulent flames. *Proceedings of the Combustion Institute*, 12:1093–1102, 1969.